

THESIS

INVESTIGATION OF SURFACE INTERACTIONS OF PYRAZINAMIDE AND
PYRAZINOIC ACID WITH SYNTHETIC AND NATURAL LIPID MEMBRANE MODEL
SYSTEMS

Submitted by

Nathaniel Gasparovic

Department of Chemistry

In partial fulfillment of the requirements

For the degree of Master of Science

Colorado State University

Fort Collins, Colorado

Fall 2022

Master's Committee:

Advisor: Debbie C. Crans

Chuck Henry
Elizabeth Ryan

Copyright by Nathaniel Glenn Gasparovic 2022

All Rights Reserved

ABSTRACT

INVESTIGATION OF SURFACE INTERACTIONS OF PYRAZINAMIDE AND PYRAZINOIC ACID WITH SYNTHETIC AND NATURAL LIPID MEMBRANE MODEL SYSTEMS

Pyrazinamide (PZA) is a pro-drug used in the treatment of tuberculosis. Upon administration of the drug, it is converted to its active form of pyrazinoic acid (POA) by the tuberculosis bacterium; this is believed to be the biologically active form of the drug which exerts anti-tubercular activity. However, it is generally accepted that both compounds interact with and transverse the membrane, with POA potentially functioning as a protonophore and lowering the intracellular mycobacterial pH. To investigate the interactions of PZA and POA in model membranes, we employed Langmuir monolayers to investigate the potential membrane-disrupting effects of PZA and POA on a model membrane. At physiological pH, neither PZA nor POA disrupted the membrane, although a difference in compressibility was observed. At acidic pH, POA became more disruptive but only at high, non-physiological concentrations. ^1H NMR spectroscopy of a microemulsion system was used to investigate the location of PZA and POA in the interface in different protonation states. The neutral POA species was found to preferentially reside in the interface while the charged species remained in the interfacial water. Finally, the effects of PZA and charged POA on the bilayer in liposomes were investigated. A leakage assay on fluorophore-filled liposomes showed that PZA and POA do not induce leakage in the membrane at physiological conditions.

TABLE OF CONTENTS

ABSTRACT.....	ii
1. Introduction.....	1
2. Results & Discussion.....	4
2.1. Compression Isotherms of Langmuir Monolayers.....	4
2.1.1. PZA vs POA _C at pH 7.4.....	4
2.1.2. pH Affects the Association of PZA with Langmuir Monolayers.....	5
2.1.3. Compression Modulus Analysis at pH 7.4.....	7
2.2. ¹ H NMR Studies of PZA and POA.....	9
2.2.1. ¹ H NMR Measurements of PZA in AOT Reverse Micelles.....	9
2.2.2. ¹ H NMR Measurements of POA in AOT Reverse Micelles.....	10
2.3. Liposome Leakage Assay to Determine Ability of PZA and POA to Disrupt a Bilayer Membrane.....	13
2.4. Implications and Future Directions.....	15
3. Materials and Methods.....	17
3.1. General Materials and Methods.....	17
3.2. Preparation of Solutions for Langmuir Monolayer Studies.....	17
3.3. Formation and Compression of Langmuir Monolayers.....	18
3.4. Compression Modulus Analysis of Langmuir Monolayers.....	19
3.5. Preparation of Solutions for Reverse Micelles.....	19
3.6. ¹ H NMR Spectroscopic Studies of Reverse Micelles.....	20
3.7. Dynamic Light Scattering (DLS).....	20
3.8. Preparation of Buffers for Liposomes.....	21
3.9. Preparation of Liposomes.....	21
3.10. Fluorescence Leakage Assay of Liposomes.....	21
4. Conclusions.....	23
5. References.....	24

1. INTRODUCTION

Pyrazinamide (PZA) and pyrazinoic acid (POA) (**Figure 1**) are two important small molecules involved in the treatment of tuberculosis (TB), caused by *Mycobacterium tuberculosis* (*Mtb*).^{1,2,3} PZA is a pro-drug metabolized into POA by the *Mtb* cell.^{4,5} This metabolism occurs through the following process: first, the PZA must enter the *Mtb* cell where it is then converted into pyrazinoate by the enzyme pyrazinamidase (PZAase). The pyrazinoate then leaves the *Mtb* and reenters the surroundings where it is protonated into pyrazinoic acid. The now protonated POA, acting as a protonophore, reenters the *Mtb* over a pH gradient and deprotonates, depositing the proton within the cell, which then exerts anti-tubercule activity. In order to exhibit this anti-TB activity, POA must be able to enter the *Mtb* cell and therefore might associate with the plasma membrane in some capacity, although it is unknown how. As such, we wanted to explore the location and association of PZA and POA with model membranes as well as their potential to disrupt the membrane. Due to the pH-dependent nature of POA,^{4,6} we refer to the neutral (protonated) species POA_N and the charged (deprotonated) species POA_C. To investigate, we employed three different model membranes: Langmuir monolayers, reverse micelles (RM), and liposomes.

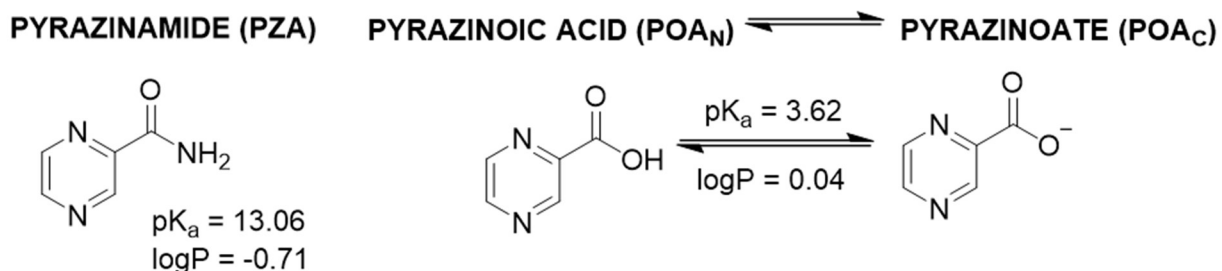


Figure 1. The structures and pK_a values of A) pyrazinamide (PZA) and B) pyrazinoic acid (POA_N)/pyrazinoate (POA_C). The pK_a values for PZA and POA are predicted values from www.chemicalize.com. The $\log P$ values are predicted values from www.molinspiration.com.

Langmuir monolayers are self-assembled monolayers at the air-water interface which can be used to study the location and association of small molecules within a phospholipid model membrane.^{7,8} In this manuscript, the phospholipids dipalmitoylphosphatidylcholine (DPPC) and dipalmitoylphosphatidylethanolamine (DPPE) were used to form monolayers. DPPC is commonly used due to the distinct phases exhibited during compression, giving information on packing.⁹ However, DPPC is a eukaryotic phospholipid and is therefore not present in *Mtb*.¹⁰ Thus, we also used DPPE, as ethanolamine phospholipids are much more plentiful in bacterial membranes.^{11,12} We expect POA_N will be located in the interface, potentially disrupting the phospholipid packing while POA_C and PZA will remain either in the water or near the interface without disrupting packing of the monolayer. As opposed to the usual biochemistry terminology, in Langmuir studies the “disruption” of membranes refers to any changes in the membrane, not solely damage, and thus it will be used in that manner in any sections referring to Langmuir monolayer studies. In non-Langmuir studies however, disruption will refer to damages to the membrane.

While Langmuir monolayers give general information on location, we wanted to obtain molecular information regarding the location of POA and PZA in the interface. NMR of RMs provides an opportunity to obtain the desired molecular information.¹³ RMs are a microemulsion wherein a nanodroplet of water is encased in surfactant and suspended in a non-polar solvent.^{14,15} There are several surfactant/solvent systems available and we used the well-characterized aerosol-OT (AOT)/isooctane system.¹⁵ We previously used the AOT/isooctane system to determine the location of benzoic acid and its conjugate base, benzoate, in the interface with 1D and 2D ¹H NMR.¹⁶ It was found that benzoic acid resided within the interface while benzoate remained in the water pool. We expect to obtain similar results using 1D NMR, where POA_N will reside within the interface while POA_C will remain in the water.

To further investigate association as well as potential disruption of the bilayer as opposed to the monolayer, we utilized large unilamellar vesicles (LUV) composed of phosphatidylcholine (POPC).¹⁷ LUVs may be loaded with a fluorescent dye, such as 5(6)-carboxyfluorescein (CF), at self-quenching concentration.¹⁷ If the bilayer is disrupted, then CF will be released into the bulk solution and fluoresce. We expect that the only molecule in this study that might induce leakage will be POA_N, as it will likely reside within the interface, giving it greater potential to disrupt the membrane than a molecule that remains within the water. We hypothesize that, by using this combination of Langmuir monolayers, 1D NMR of RMs, and leakage assays, we will find that i) PZA will not associate with the interface as it is a pro-drug and has a much more negative logP than POA (**Figure 1**), ii) POA_N and POA_C will occupy different regions within the interface, and iii) POA will associate with, but not necessarily disrupt the interface.

2. RESULTS AND DISCUSSION

2.1 COMPRESSION ISOTHERMS OF LANGMUIR MONOLAYERS

2.1.1 PZA VS POA_C AT pH 7.4. The associations of PZA and POA_C with phospholipids were determined via compression isotherm at concentrations of 0.1 mM, 1 mM, and 10 mM (pH 7.40 ± 0.02) in Langmuir monolayers prepared from dipalmitoylphosphatidylcholine (DPPC) and dipalmitoylphosphatidylethanolamine (DPPE) (**Figure 2**). Neither DPPC nor DPPE compression isotherms exhibited any change in area or shape upon exposure to PZA or POA_C. This is consistent with the hypothesis that POA_C enters the interface, but that the effect is weak. Compression isotherms suggest that PZA and POA, however, do not disrupt the membrane. Though, considering that POA has different protonation states, the effects of pH on the association of the different species with the monolayer were investigated.

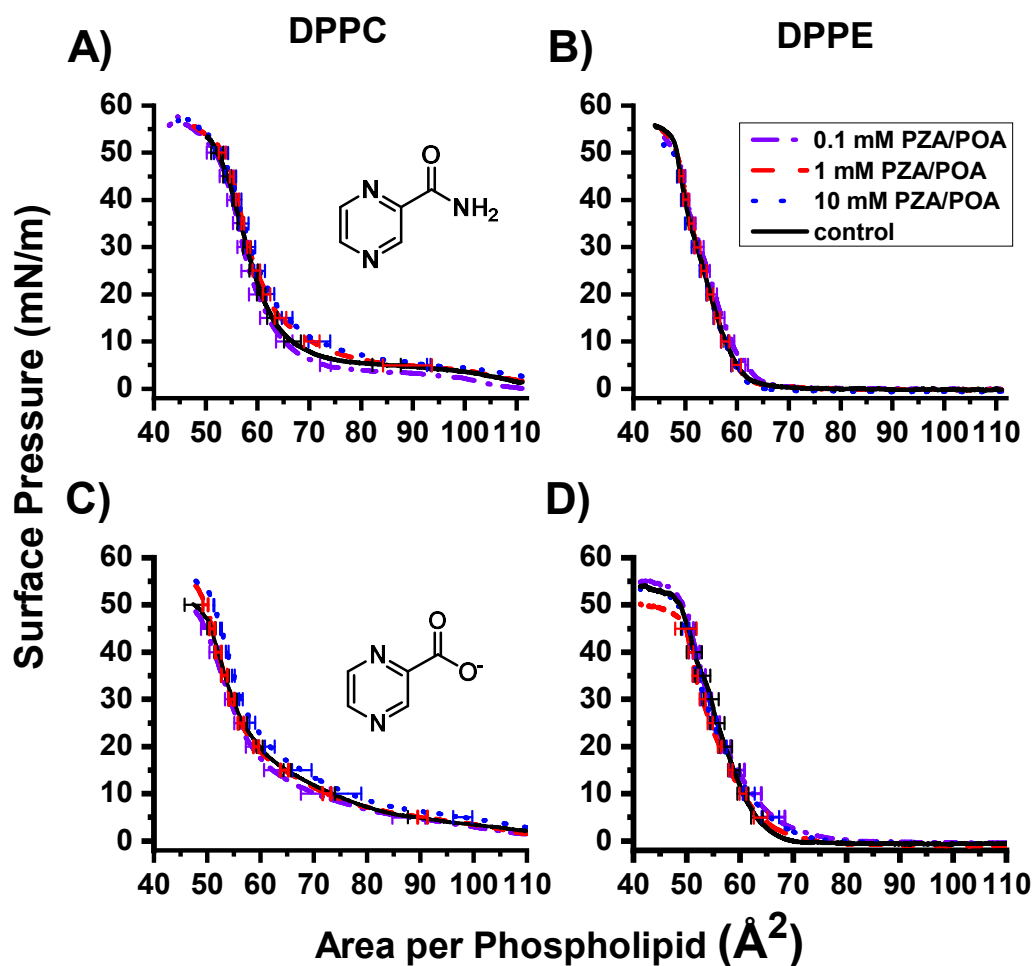


Figure 2. Compression isotherms of DPPC (left column) or DPPE (right column) with either PZA (A and B) or POAc (C and D) as the analyte at $\text{pH } 7.4 \pm 0.02$. Black solid curves represent control monolayers with no analyte present, blue dotted curves represent monolayers with 10 mM PZA/POAc present, red dashed curves represent monolayers exposed to 1 mM PZA/POAc, and purple dash-dot curves represent monolayers exposed to 0.1 mM PZA/POAc. Each curve is the average of triplicate measurements. Error bars are the standard deviation of the area and are reported at every 5 mN/m of surface pressure.

2.1.2 pH AFFECTS THE ASSOCIATION OF POA WITH LANGMUIR MONOLAYERS. Compression isotherms were obtained of POA at pH 5, where there should be a mixture of both POAN and POAc, and pH 3, where the majority molecules should be POAN (**Figure 3**). With DPPC, we see an overall expansion of the monolayer at all concentrations, unlike the similar responses at pH 7.4 shown above. At physiological surface pressure (30-35 mN/M)¹⁸

and a pH of 5, DPPC is slightly condensed. However, the differences are small enough that there may not be any physiological implications. There is also an expansion of at least 2 \AA^2 at physiological surface pressure for DPPE monolayers. As with the DPPC monolayers, this is likely not an indication of more than a moderate association.

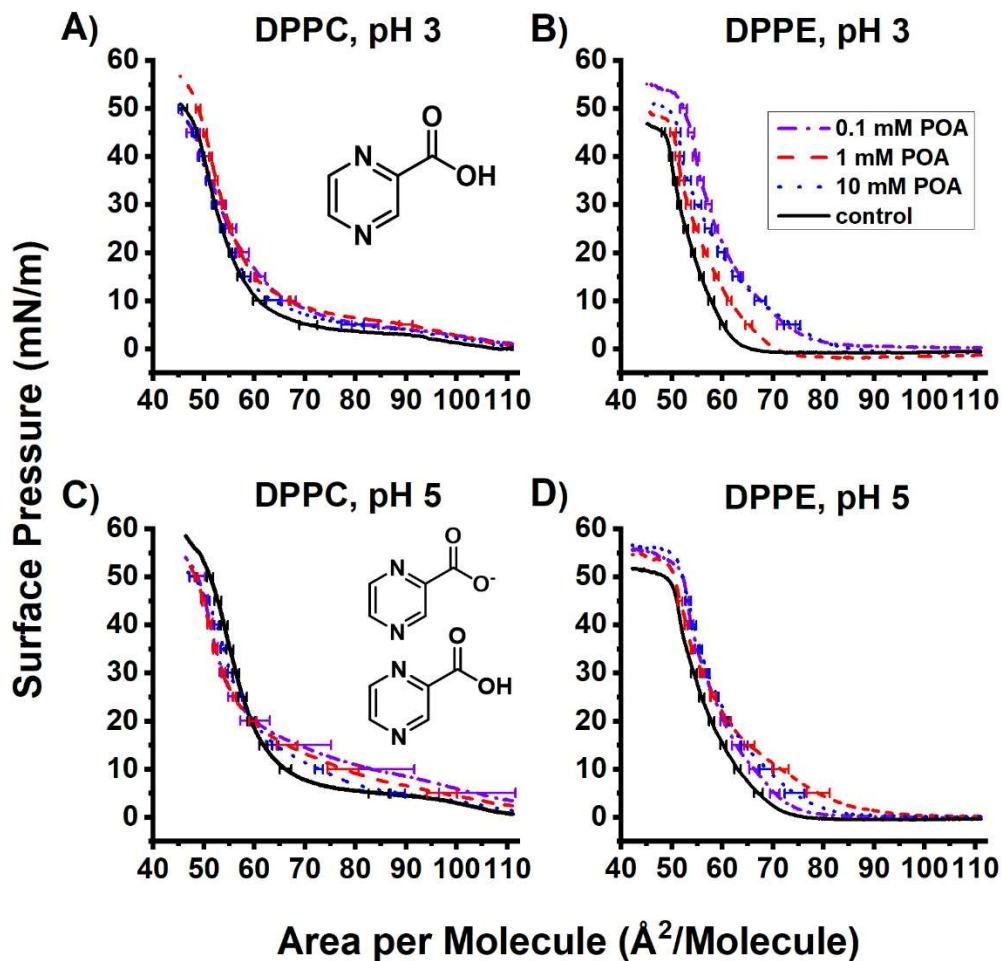


Figure 3. Compression isotherms of DPPC (left column) or DPPE (right column) with the subphase at either pH 3 (A and B) or pH 5 (C and D). Structures of species present are provided. Solid black curves represent control monolayers with no POA present, blue dotted curves represent 10 mM POA, red dashed curves represent 1 mM POA, and purple dash-dot curves represent 0.1 mM POA. Each curve is the average of at least three replicates. Error bars are the standard deviation of the area.

At pH 3, there is some expansion of the DPPC monolayer, although overall the response is moderate just like at pH 5 and pH 7.4. This can be interpreted as POA_N residing within the interface, but not causing any significant differences in packing. This is in line with findings that POA is a protonophore and would have some association with, but not disrupt, the model membrane enough to measure.¹⁹ Protonophores, as previously described, are able to permeate the membrane without disrupting the bilayer. Therefore, we propose that POA's ability to interact without damaging the membrane is in line with this definition.

POA is charged at pH 7.4 and neutral at pH 3, where we see a disruptive effect on the area of DPPE at 0.1 mM and 10 mM concentrations of POA_N. A much smaller effect is observed in DPPC curves. The possibility that these expansive effects are due to the pH instead of the protonation state of POA was ruled out by comparison with the monolayer without any POA. Furthermore, since the pK_a values of both DPPC and DPPE are below two,²⁰ any observed differences are most likely due to the POA protonation states as opposed to the protonation states of the phospholipids.

2.1.3 COMPRESSION MODULUS ANALYSIS AT pH 7.4. Compression moduli were calculated from the isotherms to assess monolayer compressibility and to confirm phase transitions in DPPC (**Figure 4**). An increase in the compression modulus relative to the control indicates increased rigidity of the monolayer, while a decrease indicates that the monolayer is becoming more elastic. When exposed to PZA, DPPC did not show a disappearance of the gas-liquid phase transition, indicating that there is not likely a rearrangement of the monolayer. The monolayers exposed to 0.1 mM and 10 mM exhibit little to no difference in compressibility while treatment with 1 mM PZA showed increased elasticity. For DPPE, PZA showed no effect except at 10 mM, where the monolayer becomes more elastic. Together, the compression moduli of DPPC and DPPE

exposed to PZA may indicate that it makes monolayers more tolerant to compression despite observing no difference in the compression isotherms. A difference in the modulus but not the isotherm suggests that PZA is at the interface but does not preferentially reside within the interface at physiological pH.

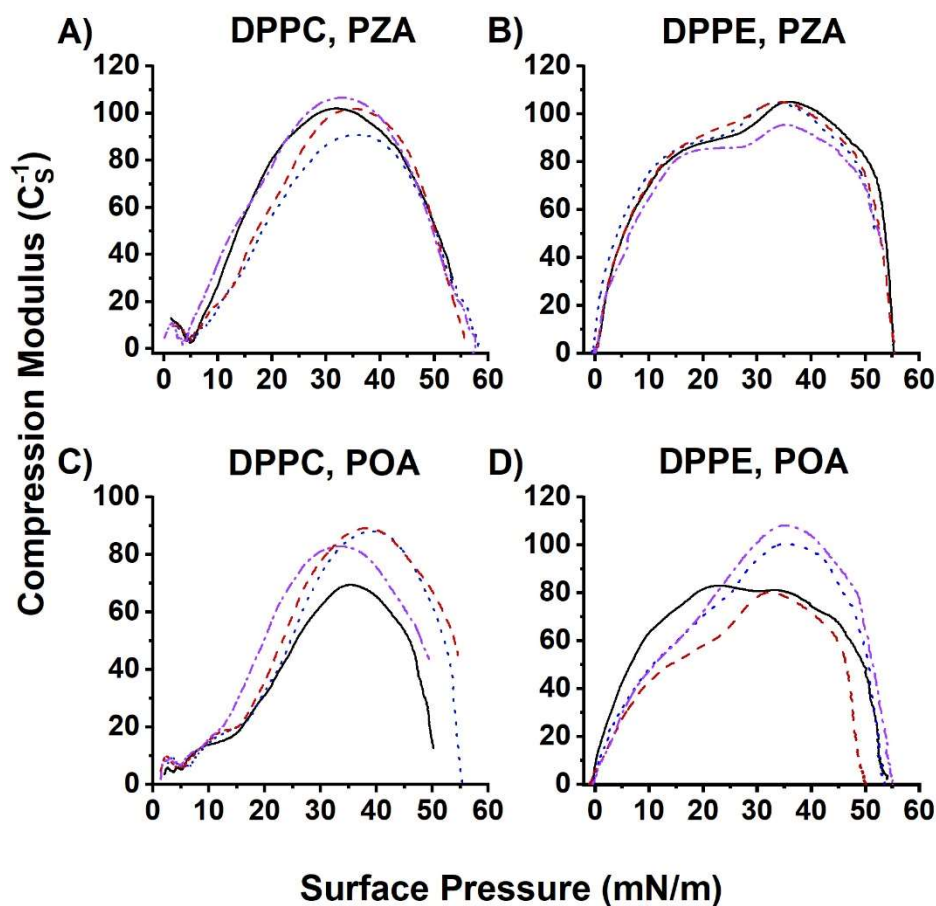


Figure 4. Compression moduli of DPPC (left column) or DPPE (right column). Black curves represent phospholipid controls, blue dotted curves represent 10 mM of probe molecule, red dashed curves represent 1 mM of probe molecule, and purple dash-dot curves represent 0.1 mM probe molecule. Curves are the average of at least three replicates.

These moduli show that, while it may not increase the area or phase transitions of the monolayer at pH 7.4, POA_C is making the monolayer less tolerant to changes due to compression. In conjunction with observations of compression isotherms, this shows that it is likely that POA_C

is at the interface but only slightly penetrates it at pH 7.4. The increased rigidity is contrary to the effects of PZA. To investigate this further, we carried out an NMR analysis.

2.2 ^1H NMR STUDIES OF PZA AND POA

2.2.1 ^1H NMR MEASUREMENT OF PZA IN AOT REVERSE MICELLES. PZA was added to a series of reverse micelles (RM) of varying size prepared from NaAOT in isooctane and with w_0 ranging from 8 to 20. The full ^1H NMR spectra of 100 mM POA in 0.75 M AOT in isooctane is shown in the Supplemental Information (**Figures S2.1, S2**) but in **Figure 5** we show only the aromatic region. The fact that the RM ^1H NMR spectra of PZA change significantly from the aqueous solution is clear evidence that PZA interacts with the interface. H_a in 100% D_2O had a chemical shift of 9.22 ppm (**Figure 5**) but when PZA solutions are placed in RMs, H_a shifts downfield as the RMs size is reduced. Downfield shifts have previously been associated with location in the interface²¹ and would suggest that H_a is associated with the interface, possibly near the AOT headgroup. In contrast, H_b is a doublet at 8.84 ppm and shifts upfield as the RM size reduces. This implies that H_b is located further up in the interface, likely in the AOT tails as reported previously.^{21,22} Similarly, H_c at 8.78 ppm shifts upfield as the RM size reduces, showing that this proton is located in a similar environment as that of H_b . Based on the differences in the shifting, we suggest that H_a and the amide functionality are facing the polar headgroup of AOT (towards the bulk water pool), whereas H_b and H_c are oriented toward the hydrophobic tail groups. The spectra of PZA were also recorded at different pD values. However, since there is no acidic proton, no significant change in chemical shifts was observed (**Figure S3.2**).

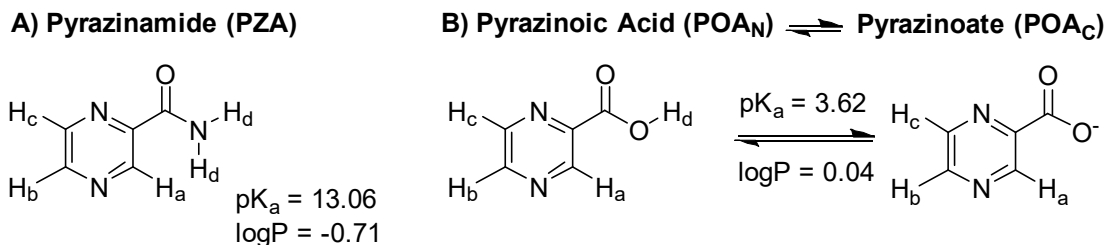


Figure 5. Proton labels to be used in ^1H NMR spectra for PZA & POA

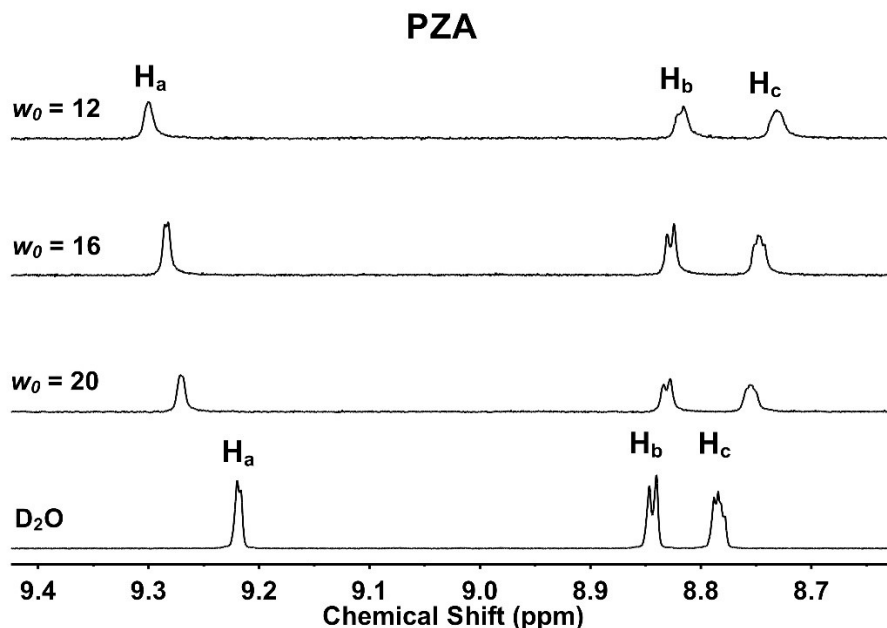


Figure 6. ^1H NMR spectra of 100 mM PZA in 0.75 M NaAOT/isooctane reverse micelles (size w_0 8-20) and D_2O . Proton labels are defined in **Figure 5**.

The spectra of PZA were also recorded at different pD values. However, since there is no acidic proton, no significant change in chemical shifts was observed (**Figure S3.2**).

2.2.2 ^1H NMR MEASUREMENTS OF POA IN AOT REVERSE MICELLES. Since POA has an acidic proton, ^1H NMR spectra were recorded from acidic (pD 2.16) and neutral (pD 6.96) stock solutions to represent POA_N and POA_C, respectively, in the AOT/isooctane model membrane interface system (**Figure 6**). An acidic solution of POA_N was added to a series of reverse micelles sized w_0 8-20 prepared from 0.75 M NaAOT in isooctane. When dissolved in D_2O at pD 2.16 (POA_N), the chemical shift of H_a is 9.27 ppm, H_b is at 8.84 and H_c is at 8.77 ppm (**Figure 6A**).

When a solution of POA_N was added to RMs of sizes w_0 12-20, H_a shifts upfield and H_b and H_c coalesce and shift upfield. These shifts are interpreted as POA_N residing further up in the interface and AOT tails than POA_C as opposed to residing in the water pool.

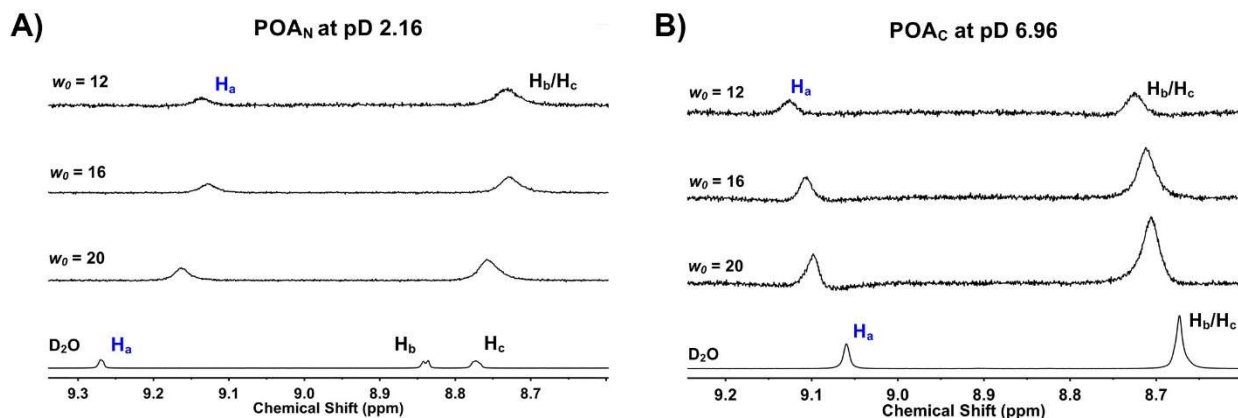


Figure 7. ¹H NMR spectra of A) 100 mM POA_N at pD 2.16 and B) 100 mM POA_C at pD 6.96 in D₂O and different sizes of 0.75 mM AOT/isooctane reverse micelles.

A solution of pD 6.96 (POA_C) was added to 0.75 M mM AOT/isooctane with w_0 ranging from 8 to 20. In aqueous solution, the ¹H NMR chemical shift of H_a appears at 9.06 ppm, significantly upfield from that observed at acidic pH (9.27 ppm). When this solution was incorporated into the RMs, the chemical shifts increased above 9.1 ppm with the peaks shifting increasingly downfield as the RM water pool becomes smaller. These observations are interpreted as the POA_C being associated with the interface but will most likely reside in or near the Stern layer. This is in line with the Langmuir monolayer studies described above where POA_C interacted with the monolayer but mainly remained in the water.

¹H NMR spectra were recorded for a series of POA solutions with varying pD values in different sizes of RM to investigate the pK_a value of the POA associated with the interface (Figure 7). There is a consistent pattern observed across different sizes, so only experiments in w_0 16 RM will be discussed (Figure S3.6). H_a shifted downfield from 9.32 to 9.12 when the pD of the stock solution rose from 1.26 to 2.16. H_a then shifted to 9.11 at pD 3.92 where it remained for the

increasing pD values. These studies demonstrated that the pK_a of POA associated with the AOT/isooctane interface is less than two. A change in the pK_a value would be anticipated if the POA was associated with the interface. Spectra recorded for the H_a proton of POA in w_0 16 and w_0 12 RMs (**Figure S3.5, Figure S3.7**) demonstrate a consistent decrease of the pK_a value when associated with the interface. In the case of POA, the pK_a change is more than one pH unit and hence consistent with the interpretation that the POA is interacting with the AOT interface.

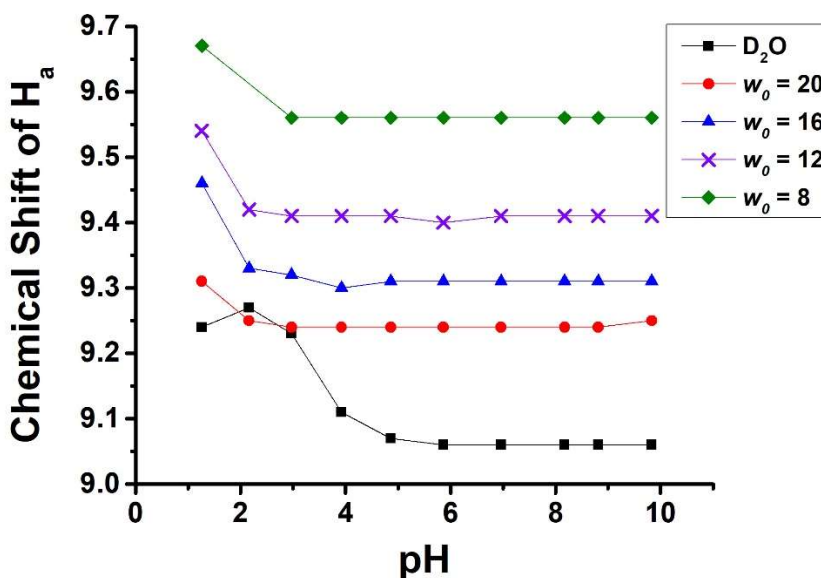


Figure 8. Chemical shifts of H_a proton in 100 mM POA plotted as a function of pH. In RMs prepared from 0.75 M AOT/isooctane reverse micelles of varying sizes: red circles represent w_0 20, blue triangles represent w_0 16, purple X's represent w_0 12, green diamonds represent w_0 8, and black squares represent D_2O . The 1H NMR spectra of the H_a proton of POA in RMs sizes w_0 12 and w_0 16 and w_0 20 are provided in Supplemental Information (**Figures S3.4, S3.6, S3.8**).

Previously, several studies observed that different acids, such as the aforementioned benzoic acid and dipicolinic acid, had a decreased pK_a value upon addition to RMs.^{16,22,23} These acids were found to penetrate the AOT interface using a variety of techniques such as 1H NMR, ^{51}V NMR, Langmuir monolayers, RMs, and other model membrane techniques.^{21,23,24,25, 26} Previously, anilinium was found to change the pK_a value upon penetration of the AOT-reverse micelle interface,²⁷ but these changes are smaller than the differences observed here. We conclude

that the large reduction in pK_a is also consistent with placement within the interface. In this case the placement may be further up into the interface since there is a large change in the environment, causing a greater change in the pK_a value.

While the 1D ^1H NMR studies provide several lines of evidence and suggestions for where POA_N and POA_C are located, additional evidence providing exact information pertaining to where in the interface each of these species are located is desirable. ^1H - ^1H 2D NOESY studies in the past have provided such information documenting how far up in the interface substrates have been found to penetrate. We have attempted these studies, but PZA and POA are sparingly soluble and, as such, we have had difficulty detecting off-diagonal cross peaks of POA in ^1H - ^1H 2D NOESY spectra and were not able to accurately determine how far up into the interface the POA_N and POA_C derivatives penetrated.

2.3 LIPOSOME LEAKAGE ASSAY TO DETERMINE ABILITY OF PZA AND POA TO DISRUPT A BILAYER MEMBRANE

Combined, the Langmuir monolayer and NMR studies suggest that POA_N and POA_C are associating weakly with the interface. Studies in cellular systems show that POA is a protonophore²⁸ and able to transport H^+ across a membrane equilibrating an existing pH potential.²⁹ Hence it is believed that POA_N and POA_C are both able to traverse membranes without causing disruption. In the following experiments, we aimed to confirm that neither POA_N nor POA_C are able to disrupt the membrane. In the following, we test the ability of PZA and POA to cause leakage in a bilayer by loading a large unilamellar vesicles (LUV) prepared from L- α -phosphatidylcholine lipids (16:0, 18:1 PC from egg yolk) with a fluorophore to determine whether the lipid bilayer is compromised in the presence of the additive.

Specifically, LUVs encapsulating self-quenching 5(6)-carboxyfluorescein (CF) were exposed to varying concentrations of PZA or POA with the objective to determine if the additive is capable of disrupting the liposomal membrane. If the membrane is disrupted, the self-quenching dye is released and an increase in fluorescence intensity is observed.^{30,31} A positive control experiment was done in which concentrations varying from 0-0.5% of Triton X-100 were added to test validity of the assay (**Figure 9A**). This experiment serves as a control experiment, as Triton X-100 is known to penetrate and disrupt lipid bilayers, leading to the release of dye when the lipid bilayer is compromised. Increasing the percent volume of Triton resulted in a linear increase in fluorescence with an $R^2 = 0.92$, thus validating the method (**Figure 9A**).

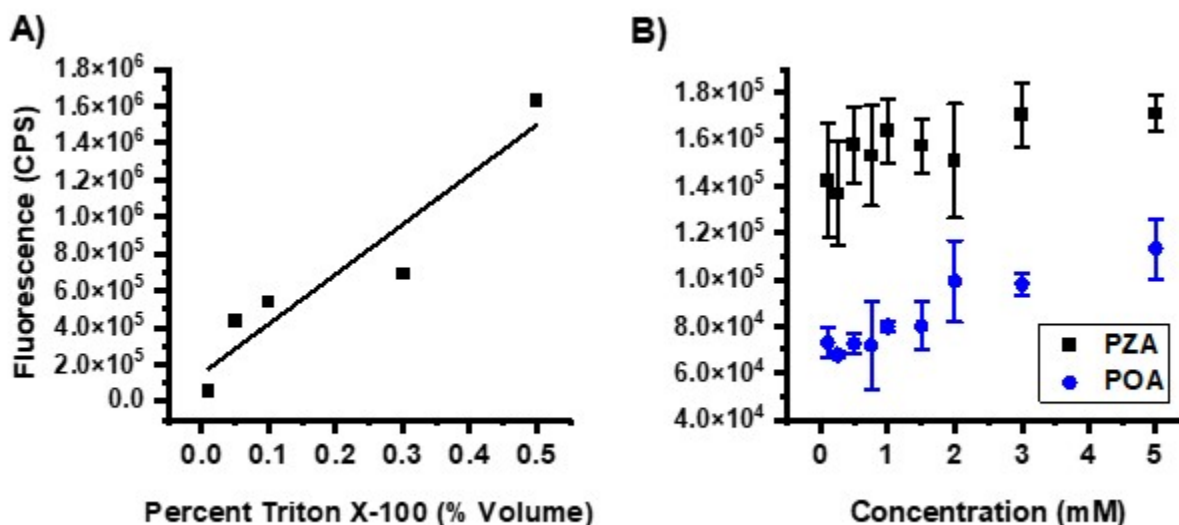


Figure 9. Induced CF leakage studies of LUVs prepared from L- α -phosphatidylcholine with A) Triton X-100 or B) PZA and POA. A) Fluorescence vs. percent Triton X-100 fitted to a linear regression model ($R^2 = 0.92$). B) Fluorescence vs concentration of PZA (black squares) or POA (blue circles). It should be noted that the scale of B is 10-fold lower than that of Panel A. Error bars are the standard deviation of triplicate measurements. A bar graph with the average fluorescence intensity of experimental groups is provided in the Supplemental Information (**Figure S4.2**).

Addition of 1-5 mM PZA and POA overall did not induce any appreciable fluorescence, as the change in fluorescence within the biological range was within a magnitude of the zero (**Figure 9B**). It should also be noted that the maximum fluorescence observed in the Triton control experiment is tenfold higher than that of any sample exposed up to 5 mM of PZA or POA. This observation supports the conclusion that negligible fluorescence is resulting from adding up to 5 mM PZA or POA to a LUV documenting the integrity of the lipid bilayer in the LUV. Since the bilayer is not compromised, this conforms to our studies with Langmuir monolayers and RMs and suggests that cells in a biological system will also remain intact and not cause disorganization of a biological membrane bilayer.

2.4 IMPLICATIONS AND FUTURE DIRECTIONS

Table 1. Summary of the methods used in the research, what they were used to find, and what conclusions were found through their usage.

Technique	Model Membrane Used	What was it used for?	Conclusions
Langmuir trough	Langmuir monolayer	Location within the membrane	1. PZA & POA _N reside at membrane but do not disrupt it 2. POA _C resides at membrane but only slight penetrates
¹ H NMR	Reverse micelle	Detailed chemical information about location within the membrane	1. PZA resides in tail region 2. POA _N resides in headgroup & tail 3. POA _C resides in headgroup & water pool
Leakage Assay	Large unilamellar vesicle	Association with & disruption of the membrane	Bilayer of cells not disrupted by PZA/POA

Much like benzoic acid and benzoate, POA_N and POA_C reside in different locations of the membrane as suggested by several lines of evidence. Specifically, POA_N resides further up in the hydrophobic part of the interface while POA_C resides in the hydrophilic Stern layer. This observation is consistent with the possibility that POA, like benzoic acid, is able to behave as a protonophore in a bilayer when there is a pH gradient across the membrane. These results suggest that PZA, POA_N and POA_C do not compromise the organization of the lipid bilayer even though we have shown that they are able to incorporate themselves with a membrane interface. Hence, although POA behaves as a protonophore, such disruption of the pH gradient is not due to disruption of the membrane but more likely due to the transport of POA_N across the membrane and delivery of the acidic proton. Combined, these studies confirm our hypothesis that *the association of PZA and POA with lipid monolayers and bilayers does not disrupt the phospholipid bilayer but instead leaves the membrane intact.*

In the future, work can be done to confirm the results gained from the leakage assay but applied to prokaryotic cells, such as *Mtb*. The leakage assay test has currently only been done utilizing POPC, which is found in eukaryotic cells and thus not present in *Mtb*. To remedy this it can be repeated utilizing dipalmitoylphosphatidylethanolamine which is similarly structured to POPC but is found in prokaryotic cells.

3. MATERIALS AND METHODS

3.1 GENERAL MATERIALS AND METHODS. The following materials were used without further purification: chloroform ($\geq 99.5\%$), monosodium phosphate ($\geq 99.0\%$), disodium phosphate ($\geq 99.0\%$), citric acid ($\geq 99.5\%$), sodium citrate dihydrate ($> 99\%$), sodium chloride ($\geq 99.0\%$), sodium hydroxide ($\geq 98\%$), hydrochloric acid (37%), 2-pyrazincarboxamide (pyrazinamide, PZA, $\geq 98.0\%$), 2-pyrazincarboxylic acid (pyrazinoic acid, POA, 99%), 2,2,4-trimethylpentane (isooctane, 99.8%), 2,2-dimethyl-2-silapentane-5-sulfonate sodium salt (DSS, 97%), L- α -phosphatidylcholine (16:0, 18:1 PC, egg yolk, Type XVI-E, $\geq 99\%$), 5(6)-carboxyfluorescein ($\geq 95\%$), and HEPES ($\geq 99.5\%$), were all purchased from Sigma-Aldrich. The phospholipids dipalmitoylphosphatidylcholine (16:0 PC, DPPC, 99%) and dipalmitoylphosphatidylethanolamine (16:0 PE, DPPE, 99%) were purchased from Avanti Polar Lipids as pure lyophilized powder. Deuterium oxide (D_2O , $\geq 99\%$) was purchased from Cambridge Isotope laboratories. Aerosol-OT (AOT, dioctyl sulfosuccinate sodium salt, $\geq 99.0\%$) was purchased from Sigma Aldrich and purified with charcoal as previously described.²⁵ Distilled deionized (DDI) water was obtained by filtering distilled water through a Millipore water purification system, obtaining a resistance of 18.2 M Ω .

The Langmuir monolayers were studied using a Kibron μ Trough XS (stainless steel) equipped with a Teflon ribbon barrier. All 1H NMR experiments were performed using a 400 MHz Varian NMR spectrometer. Dynamic light scattering studies were performed on a Malvern Zetasizer ZS equipped with a 633 nm red laser. Fluorescence studies were done on a Horiba Jobin-Yvon FluoroLog-3 where the cuvette was attached to the light source and detector by fiber optic

cables. All pH and pD values were obtained with a Thermo Orion 2 Star pH meter (pH = pD + 0.4). Liposome extrusion was done with a mini-extruder purchased from Avanti Polar Lipids.

3.2 PREPARATION OF SOLUTIONS FOR LANGMUIR MONOLAYER STUDIES.

The subphase consisted of 20 mM sodium phosphate-citrate buffer. Buffers were adjusted to pH 3, 5, or 7.4. Solutions of PZA or POA were created by dissolving an appropriate amount of solid into 250 mL of buffer to create a 10 mM solution (0.3078 g PZA, 0.3105 g POA). Solutions of 1 mM and 0.1 mM were created by diluting from the 10 mM solutions. PZA solutions were brought to pH 7.40 ± 0.02 with 1 M HCl or NaOH. POA solutions were adjusted to pH 3.00, pH 5.00, or pH 7.40 ± 0.02 with 1 M HCl or NaOH.

Phospholipid stock solutions were prepared by dissolving dipalmitoylphosphatidylcholine (DPPC) (0.018 g, 0.025 mmol) or dipalmitoylphosphatidylethanolamine (DPPE) (0.017 g, 0.025 mmol) in 25 mL of 9:1 chloroform/methanol (v/v) for a final concentration of 1.0 mM phospholipid.

3.3 FORMATION AND COMPRESSION OF LANGMUIR MONOLAYERS.

The buffered aqueous subphase consisted of 50 mL of 20 mM sodium phosphate-citrate buffer (pH 3.00, 5.00, 7.40) in DDI water (18.2 M Ω). The subphase surface was cleaned via vacuum aspiration until a compression of the subphase resulted in a surface pressure that was consistently 0.0 ± 0.5 mN/m throughout compression. A total of 20 μ L of phospholipid stock solution (20 nmol of lipid) was then added to the surface of the subphase in a dropwise manner using a 50 μ L Hamilton syringe. The monolayer was allowed to equilibrate for 15 minutes.

The equilibrated monolayer was compressed from two sides with a total speed of 10 mm/min (5 mm/min from each side). The temperature was maintained at 25 °C using an external water bath. The trough plate was washed three times with isopropanol, then three times with

ethanol, then rinsed with DDI water (18.2 M Ω) before each experiment. The ribbon barrier was rinsed with isopropanol followed by ethanol and then water. The surface tension was monitored via Wilhemy plate technique in which a steel wire was used as the probe instead of a plate. The surface pressure was calculated from the surface tension using **Equation 1**, where π is the surface pressure, γ_0 is the surface tension of water (72.8 mN/m), and γ is the surface tension at a given area per phospholipid after the monolayer has been applied.

$$\pi = \gamma_0 - \gamma \quad (1)$$

Each compression isotherm experiment consisted of at least three replicates. The averages of the area per phospholipid and the standard deviation at every 5 mN/m were calculated using Microsoft Excel. The worked-up data were then transferred to Origin 2021 to be graphed.

3.4 COMPRESSION MODULUS ANALYSIS OF LANGMUIR MONOLAYERS. The compression modulus of each average was calculated according to **Equation 2**, where C_s^{-1} is the compression modulus, A is the area per molecule (\AA^2), and π is the surface pressure.

$$C_s^{-1} = -A \left(\frac{d\pi}{dA} \right)_T \quad (2)$$

The first derivative of the surface pressure with respect to temperature was calculated in Origin 2021 and smoothed with a second degree polynomial Savitsky-Golay function (350 points per window). The derivative was then multiplied by the negative area and graphed versus surface pressure in Origin 2021.

3.5 PREPARATION OF SOLUTIONS FOR REVERSE MICELLES. Solutions for studies by ^1H NMR are done in D_2O , therefore the measured pH values are adjusted to pD with $\text{pD} = \text{pH} - 0.4$.³² Stock solutions of approximately 100 mM PZA or POA were made by dissolving 0.123 g PZA or 0.124 g POA in 20 mL of D_2O . Stocks were then aliquoted into 2 mL samples. Each sample

was brought to a different pD ($\text{pH} = \text{pD} + 0.4$) with 0.1 or 1 M DCl and/or NaOD. Each pD was within the range of 1.2 to 10 and were used to determine the pK_a .

A 750 mM stock solution of purified AOT in isooctane was prepared by dissolving 8.34 g (18.8 mmol AOT) in 25 mL isooctane. This mixture was sonicated and then allowed to equilibrate to ambient temperature. Appropriate amounts of pD-adjusted PZA or POA solution in D_2O were added to AOT/isooctane solution samples of sizes w_0 12, w_0 16, and w_0 20, where $w_0 = [\text{H}_2\text{O}]/[\text{AOT}]$. These samples were vortexed for ~ 1 minute until clear, indicating that the microemulsions had formed.

3.6 ^1H NMR SPECTROSCOPIC STUDIES OF REVERSE MICELLES. One-dimensional (1D) ^1H NMR spectra of PZA and POA were measured in D_2O and RMs and obtained using standard parameters (1 s relaxation time, 25°C , and 45° pulse angle).²⁵ The determination of pK_a values were done by recording a series of spectra at different pH values and plotting the chemical shifts as a function of pD. The data is shown in the Supplemental Information. Corresponding studies were done in RM as well and the data is presented.

Aqueous spectra were referenced to DSS. RM spectra were referenced to the internal isooctane methyl peak at 0.90 ppm corresponding to previously recorded chemical shifts in reference to the signal of trimethylsilane at 0 ppm.^{22,25,33}

3.7 DYNAMIC LIGHT SCATTERING (DLS). DLS experiments were done to verify that the RMs were formed using methods described previously.²⁵ RMs were prepared as above. The 1 mL aliquot was then diluted in 5 mL of isooctane and vortexed for ~ 2 minutes to break up aggregates. The DLS cuvette was rinsed three times with isooctane, then three times with the sample before each reading. Samples were allowed 15 minutes to equilibrate at ambient

temperature before measurements were recorded. Each reading consisted of 15 measurements with each measurement consisting of 10 scans. The average result was recorded.

3.8 PREPARATION OF BUFFERS FOR LIPOSOMES. The following were based on Jimah *et al.* 2017.³² In brief, the carboxyfluorescein (CF) buffer was prepared by dissolving 0.596 g HEPES (50 mM), 0.146 g NaCl (50 mM), and 1.88 g of 5(6)-carboxyfluorescein (100 mM) into 50 mL of DDI H₂O. The buffer was then brought to pH 7.4 with 1 M NaOH and 1 M H₂SO₄. Column buffer was prepared by dissolving 5.96 g HEPES (100 mM) and 1.46 g NaCl (100 mM) in 250 mL of DDI H₂O. The buffer was then adjusted to pH 6.5 with 1.0 M NaOH and 1 M H₂SO₄.

3.9 PREPARATION OF LIPOSOMES. Lipid cakes were prepared by dissolving 0.20 g (250 μmol) of L- α -phosphatidylcholine in 25 mL of chloroform in a 100 mL round bottom flask. The lipid solution was then dried by removing the solvent with a rotary evaporator. After all excess solvent was removed, the lipid cake was then rehydrated in 5.2 mL of CF buffer to create a 50 mM solution of lipid suspended in buffer. The round bottom flask was then agitated in a 55 °C water bath for one hour and the rehydrated solution of lipids was extruded eight times through a 0.1 μm filter to create large unilamellar vesicles. Excess CF was removed by running the sample through a size-exclusion column of Sephadex G-50 that was incubated with column buffer for a minimum of 12 hours.

3.10 FLUORESCENCE LEAKAGE ASSAY OF LIPOSOMES. Liposomes were diluted in a 1:8 ratio with column buffer to make solutions of appropriate concentration to measure small increases in fluorescence as induced by membrane-disruptive drugs. Increasing amounts of 10 mM PZA or 10 mM POA stock solutions made in column buffer (pH 6.5) were added up to 5 mM. Exact amounts of PZA or POA solution added to the liposomal solution are detailed in Supplemental Information (**Table S4.1**). Varying concentrations of the surfactant Triton X-100

were used as a positive control for fluorescence-induced by membrane leakage, as Triton X-100 is known to destabilize membrane bilayers.³⁴ Samples were allowed to incubate for one hour before fluorescence was measured in triplicate. Data was collected with $\lambda_{\text{ex}} = 492 \text{ nm}$ and $\lambda_{\text{em}} = 517 \text{ nm}$.

4. CONCLUSIONS

The membrane interactions of PZA and POA were investigated to determine if their association is able to disrupt a lipid bilayer, and their physicochemical properties are consistent with the designation of POA as a protonophore for *M. tuberculosis*.⁴ Langmuir monolayer studies shows that PZA has little to no association with the interface, while POA_C slightly associates with the interface. POA_N showed moderate expansion of the monolayer, consistent with the neutral species residing in the interface as opposed to the bulk water. NMR studies suggest that the neutral form of POA penetrates the interface while deprotonated and charged form of POA resides in the interfacial water layer. Furthermore, large unilamellar vesicles prepared from egg phosphatidylcholine loaded with a fluorescent dye did not show any leakage of dye, documenting that the vesicles are intact and not compromised by the presence of PZA or POA_C. These studies support the interpretation that when POA acts as a protonophore, it does not disrupt the membrane bilayer. Instead, the neutral and protonated form of POA is transported across the membrane, delivers the proton and transport deprotonated and charged POA back to equilibrate the pH potential over the membrane.

5. REFERENCES

- (1) Nijire, M.; Wang, N.; Wang, B.; Tan, Y.; Cai, X.; Liu, Y.; Mugweru, J.; Guo, J.; Hameed, H. M. A.; Tan, S.; et al. Pyrazinoic Acid Inhibits a Bifunctional Enzyme in *Mycobacterium tuberculosis*. *Antimicrob. Agents Chemother* **2017**, *61* (7), e00070-00017.
- (2) Sun, Q.; Li, X.; Perez, L. M.; Shi, W.; Zhang, Y.; Sacchetti, J. C. The molecular basis of pyrazinamide activity on *Mycobacterium tuberculosis panD*. *Nat. Commun.* **2020**, *11*, 339.
- (3) Zhang, Y.; Wade, M. M.; Scorpio, A.; Zhang, H.; Sun, Z. Mode of action of pyrazinamide disruption of *Mycobacterium tuberculosis* membrane transport and energetics by pyrazinoic acid. *J. Antimicrob. Chemother.* **2003**, *52* (5), 790-795.
- (4) Fontes, F. L.; Peters, B. J.; Crans, D. C.; Crick, D. C. The Acid-Base Equilibrium of Pyrazinoic Acid Drives the pH Dependence of Pyrazinamide-Induced *Mycobacterium tuberculosis* Growth Inhibition. *ACS Infect. Dis.* **2020**, *6* (11), 3004-3014.
- (5) Zhang, Y.; Shi, W.; Zhang, W.; Mitchison, D. Mechanisms of Pyrazinamide Action and Resistance. *Microbiol. Spectr.* **2003**, *2* (4), 1-12.
- (6) Zhang, Y.; Scorpio, A.; Nikaido, H.; Sun, Z. Role of Acid pH and Deficient Efflux of Pyrazinoic Acid in Unique Susceptibility of *Mycobacterium tuberculosis* to Pyrazinamide. *J. Bacteriol.* **1999**, *181* (7), 2044-2049.
- (7) Ariga, K. Don't Forget Langmuir-Blodgett Films 2020: Interfacial Nanoarchitectonics with Molecules, Materials, and Living Objects. *Langmuir* **2020**, *36* (26), 7158-7180.
- (8) Brezesinski, G.; M öhwald, H. Langmuir monolayers to study interactions at model membrane surfaces. *Adv. Colloid Interface Sci.* **2003**, *100-102*, 563-584.

- (9) Crane, J. M.; Puts, G.; Hall, S. B. Persistence of Phase Coexistence in Disaturated Phosphatidylcholine Monolayers at High Surface Pressures. *Biophys. J.* **1999**, *77*, 3134-4143.
- (10) Fadeel, B.; Xue, D. The ins and outs of phospholipid asymmetry in the plasma membrane: roles in health and disease. *Crit. Rev. Biochem. Mol. Biol.* **2009**, *44* (5), 264-277.
- (11) Shaw, N. Lipid Composition as a Guide to the Classification of Bacteria. *Adv. Appl. Microbiol.* **1974**, *17*, 63-108.
- (12) Charkrabarti, A. Phospholipid Asymmetry in Biological Membranes: Is the Role of phosphatidylethanolamine Underappreciated? *J. Membr. Biol.* **2021**, *254*, 127-132.
- (13) Van Horn, W. D.; Ogilvie, M. E.; Flynn, P. F. Use of reverse micelles in membrane protein structural biology. *J. Biomol. NMR* **2008**, *40*, 203-211.
- (14) Crans, D. C.; Rithner, C. D.; Baruah, B.; Gourley, B. L.; Levinger, N. E. Molecular Probe Location in Reverse Micelles Determined by NMR Dipolar Interactions. *J. Am. Chem. Soc.* **2006**, *128* (13), 4437-4445.
- (15) Maitra, A. Determination of size parameters of water-Aerosol OT-oil reverse micelles from their nuclear magnetic resonance data. *J. Phys. Chem* **1984**, *88* (21), 5122-5125.
- (16) Peters, B. J.; Groninger, A. S.; Fontes, F. L.; Crick, D. C.; Crans, D. C. Differences in Interactions of Benzoic Acid and Benzoate with Interfaces. *Langmuir* **2016**, *32* (37), 9451-9459.
- (17) Bryl, K.; Kedzierska, S.; Taylor, A. Mechanism of the Leakage Induced on Lipid Model Membranes by Rz1 Lipoprotein, the Bacteriophage λ Rz1 Gene Product: A Fluorescence Study. *J. Fluoresc.* **2000**, *10* (2), 209-216.
- (18) Jones, M. N.; Chapman, D. *Micelles, Monolayers, and Biomembranes*; Wiley-Liss, Inc., 1995.

- (19) Emri, T.; Leiter, É.; Pócsi, I. Effect of phenoxyacetic acid on the glutathione metabolism of *Penicillium chrysogenum*. *J. Basic Microbiol.* **2000**, *40* (2), 93-104.
- (20) Marsh, D. *Handbook of Lipid Bilayers*; CRC Press, 2013.
- (21) Horton, D. C.; VanDerveer, D.; Krzystek, J.; Tesler, J.; Pittman, T.; Crans, D. C.; Holder, A. A. Spectroscopic Characterization of L-ascorbic Acid-induced Reduction of Vanadium(V) Dipicolinates: Formation of Vanadium(III) and Vanadium(IV) Complexes from Vanadium(V) Dipicolinate Derivatives. *Inorg. Chim Acta.* **2014**, *420* (24), 112-119.
- (22) Crans, D. C.; Trujillo, A. M.; Bonetti, S.; Rithner, C. D.; Baruah, B.; Levinger, N. E. Penetration of Negatively Charged Lipid Interfaces by the Doubly Deprotonated Dipicolinate. *J. Org. Chem.* **2008**, *73* (24), 9633-9640.
- (23) Sostarecz, A. G.; Gaidamauskas, E.; Distin, S.; Bonetti, S. J.; Levinger, N. E.; Crans, D. C. Correlation of insulin-enhancing properties of vanadium-dipicolinate complexes in model membrane systems: phospholipid Langmuir monolayers and AOT reverse micelles. *Chemistry* **2014**, *20* (17), 5149-5159.
- (24) Baruah, B.; Roden, J. M.; Sedgewick, M.; Correa, M.; Crans, D. C.; Levinger, N. E. When is Water Not Water? Exploring Water Confined in Large Reverse Micelles Using a Highly Charged Inorganic Molecular Probe. *J. Am. Chem. Soc.* **2006**, *128* (39), 12758-12765.
- (25) Peters, B. J.; Van Cleave, C.; Haase, A. A.; Hough, J. P. B.; Giffen-Kent, K. A.; Cardiff, G. M.; Sostarecz, A. G.; C., C. D.; Crans, D. C. Structure Dependence of Pyridine and Benzene Derivatives on Interactions with Model Membranes. *Langmuir* **2018**, *34* (30), 8939-8951.
- (26) Gaidamauskas, E.; Cleaver, D. P.; Chatterjee, P. B.; Crans, D. C. Effect of Micellar and Reverse Micellar Interface on Solute Location: 2,6-Pyridinedicarboxylate in CTAB Micelles and CTAB and AOT Reverse Micelles. *Langmuir* **2010**, *26* (16), 13153-13161.

- (27) Sripradite, J.; Miller, S. A.; Johnson, M. D.; Tongraar, A.; Crans, D. C. How Interfaces Affect the Acidity of the Anilinium Ions. *Chemistry* **2016**, *22* (11), 3873-3880.
- (28) Lamont, E. A.; Dillon, N. A.; Baughn, A. D. The Bewildering Antitubercular Action of Pyrazinamide. *Microbiol. Mol. Biol. Rev.* **2020**, *84* (2), e00070-00019.
- (29) Feng, X.; Zhu, W.; Schurig-Briccio, L. A.; Lindert, S.; Shoen, C.; Hitchings, R.; Li, J.; Wang, Y.; Baig, N.; Zhou, T.; et al. Antiinfectives targeting enzymes and the proton motive force. *Natl. Acad. Sci.* **2015**, *112* (51), E7073-E7082.
- (30) Liu, Y.; Liu, J. Leakage and Rupture of Lipid Membranes by Charged Polymers and Nanoparticles. *Langmuir* **2020**, *36* (3), 810-818.
- (31) Nasr, G.; Grieger-Gerges, H.; Elaissari, A.; Khreich, N. Liposomal membrane permeability assessment by fluorescence techniques: Main permeabilizing agents, applications and challenges. *Int. J. Pharm.* **2020**, *580*, 119198.
- (32) Jimah, J. R.; Schelsinger, P. H.; Tolia, N. H. Liposome Disruption Assay to Examine Lytic Properties of Biomolecules. *Bio Protoc.* **2017**, *7* (15), e2433.
- (33) Samart, N.; Beuning, C. N.; Haller, K. J.; Rithner, C. D.; Crans, D. C. Interactions of Biguanide Compound with Membrane Model Interface Systems: Probing the Properties of Antimalarial and Antidiabetic Compounds. *Langmuir* **2014**, *30* (29), 8697-8706.
- (34) Pizzirusso, A.; De Nicola, A.; Sevnik, G. J. A.; Correa, A.; Cascella, M.; Kawakatsu, T.; Rocco, M.; Zhao, Y.; Celino, M.; Milano, G. Biomembrane solubilization mechanism by Triton X-100: a computational study of the three stage model. *Phys. Chem. Chem. Phys.* **2017**, *19* (44).